The Effect of Intermolecular Interactions on Local Density Inhomogeneities and Related Dynamics in Pure Supercritical Fluids. A Comparative Molecular Dynamics Simulation Study

Ioannis Skarmoutsos, Dimitris Dellis, and Jannis Samios*

Department of Chemistry, Laboratory of Physical Chemistry, University of Athens, Panepistimiopolis 157-71, Athens, Greece

The effect of intermolecular interactions of different strength on the local density inhomogeneities in pure supercritical fluids (scfs), with different intramolecular structure, was investigated by employing molecular dynamics (MD) simulation techniques. The simulations were performed at state points along an isotherm close to the critical temperature of each system ($T_r = T/T_c = 1.03$). The molecular fluids under study have been chosen on the basis of the electrostatic character of their intermolecular interactions as follows: monatomic, dipolar and hydrogen bonding (HB), quadrupolar, and octupolar. In the case of dipolar scfs, their HB nature when present was systematically explored and related to the behavior of the created local density inhomogeneities at all densities. The results obtained reveal strong influence of the dipolar and HB interactions of the investigated systems upon the local density augmentation. We found that this effect is fairly larger in the case of the dipolar and HB fluids (H_2O, CH_3OH, and NH_3) compared to those for the non-dipolar ones (Xe, CH_4, CO_2, and N_2). In the case of sc CO_2, the dependence of the local density augmentation on the bulk density is in agreement with available experimental data as also reported previously. The estimated average number of hydrogen bonds per molecule $\langle n_{HB} \rangle$ in these HB fluids shows an analogue nonlinear trend compared to the behavior of the average coordination numbers $N_{co}(\rho)$ of a particle with bulk density. The local density dynamics of the first and second solvation shell of each fluid were further analyzed and related to our previously proposed [Skarmoutsos, I.; Samios, J. *J. Chem. Phys.* **2007**, *126*, 044503] different time-scale relaxation mechanisms. Finally, the effect of the different strength of the molecular interactions corresponding to these fluids upon the local density dynamics has also been revealed in the behavior of the predicted appropriate time correlation functions and their corresponding correlation times.

I. Introduction

During the last two decades the investigation of the physicochemical properties of supercritical fluids (scfs) has stimulated the attention of the scientific community, due to the great potential benefits of their use in chemical and industrial applications.[1–6] The peculiarity in the behavior of the properties of scfs is that they can be varied continuously and markedly from gaslike to liquidlike values with a small change in pressure or temperature.[4] This feature makes scfs attractive alternatives to liquid solvents for use in the developments of new chemical processes.

According to the results obtained from the long-lasting research efforts so far, this peculiar behavior has been attributed to distinct local density inhomogeneities (LDIs) occurring in scfs. It is pointed out that in a microscopic length scale a scf resembles an inhomogeneous medium with significant density variations in space.[4–6] These density variations tend to be maximized in the thermodynamic PVT phase space close to the critical point. In this region the fluctuations in the microscopic local density are maximized, leading to very large compressibility values. Consequently, in this compressible regime, small changes in pressure lead to large changes in density. Therefore, the density-dependent properties of scfs are also varied from gaslike to liquidlike values, causing corresponding changes in solvation processes. In general, scfs provide

the opportunity to search novel physicochemical phenomena that are obscure in conventional phases, namely the gas and liquid. In several previously reported experimental[7–39] and theoretical studies,[40–62] the importance of density inhomogeneities in the determination of scf properties has been clearly underlined. Despite the research effort on this field, however, many important questions are still subjects of debate. The answer to these questions is indispensable for a more efficient use of scfs as media in a variety of new chemical applications.

With this work, we continue our studies[61–69] on the properties of scfs and especially on the characteristics of LDIs[61,62] by searching the factors that control their behavior. Before proceeding any further, we have to mention that the distinction of density inhomogeneities in local and long-range ones has been extensively discussed in our previous works,[61,62] as well as in review articles.[4] Herein, we focus our attention upon the behavior of LDIs with density in an extended class of representative neat scfs, trying in this way to obtain more information regarding the influence of the different strength of intermolecular interactions upon them. Recently, a systematic investigation on the static and dynamical behavior of LDIs in sc H_2O[61] as well as in scfs MeOH[62] and CO_2[62] was initiated in our group, aiming to explore further this subject to increase our understanding of these phenomena. Note also that Song and Maroncelli[47] have revealed that the calculated local density augmentation (LDA) values are greater in the case of sc CHF_3 than in the non-dipolar sc ethane. These preliminary results,

2784 *J. Phys. Chem. B, Vol. 113, No. 9, 2009*

Skarmoutsos et al.

TABLE 1: Summary of the Simulated Thermodynamic State Points for Each System under Investigation

	$T/T_c = 1.03$
simulated state points	ρ/ρ_c
A	0.1903
B	0.3529
C	0.6095
D	0.8597
E	1.1441
F	1.2660
G	1.4329
H	1.5654
I	2.0000

TABLE 2: Summary of the Critical Parameters (ρ_c, T_c) for Each System upon Investigation

system	ρ_c (g/cm^3)	T_c (K)
Xe	1.1000	289.73
CH$_4$	0.1626	190.56
CO$_2$	0.4676	304.13
N$_2$	0.3133	126.19
NH$_3$	0.2250	405.40
CH$_3$OH	0.2720	512.60
H$_2$O	0.3220	647.10

which reveal some strong influence of the polarity and HB upon the intensity of the LDA effect, led us to examine further the influence of intermolecular interactions in the formation of LDIs by investigating likewise some representative scfs on the basis of their different electrostatic nature resulting from their multipole expansion. The scfs selected for study were classified as follows: monatomic, dipolar and HB, quadrupolar, and octupolar fluids. From the inert monatomic scfs, we selected to investigate sc Xe. This fluid has several important chemical applications and also has been used as a prototype system for modeling theories in intermolecular forces, hydrophobic hydration, and critical phenomena.[69] Among the dipolar fluids, we have reinvestigated the HB associated fluids sc H$_2$O and MeOH, also including sc NH$_3$. Finally, apart from the quadrupolar scfs CO$_2$ and N$_2$, we studied the octupolar sc CH$_4$ as a prototype of this class.

Stimulated by our previous studies, another objective of this work is to investigate further the influence of the intermolecular forces on the local density dynamics for the first and second solvation shell of the species in each of the aforementioned fluids with bulk density. It is also of interest here to examine the effect of the bulk density on the HB network in these scfs and to discuss further the HB features obtained in connection to the LDIs behavior and related dynamics. So, as part of an ongoing effort to obtain information on such a presumable interrelation between HB network and LDIs, we performed a complete HB analysis for scfs H$_2$O, MeOH, and NH$_3$. Note that the computational methodology employed in the present treatment has been thoroughly described in our previous studies.[61,62,66,67]

In Section II of this paper, we briefly describe the computational details of the MD simulations as well as the methodology used to calculate the properties of interest. The results and discussion are presented in Section III. Finally, Section IV contains the general conclusions and remarks drawn from the present study.

II. Computational Details

All the selected scfs were simulated in the canonical ensemble at the same reduced temperature, $T_r = T/T_c = 1.03$, and for densities in the range 0.2–2.0 ρ_c.[61,62] The simulated densities and the critical parameters of the investigated fluids are summarized in Tables 1 and 2, respectively. The simulations were carried out using 500 molecules in the central simulation box employing standard periodic boundary conditions. Trial runs with larger molecular system sizes (864) were also carried out to ensure the reliability of the results obtained. Note that the bulk thermodynamic results from these complement MD runs were converged to those corresponding to 500 molecules. Each simulation was extended to 350 ps to achieve equilibrium, starting from an initial fcc configuration, and the properties of

the system were evaluated in subsequent simulations with durations of 500 ps after equilibration.

In all simulations the equations of motion were integrated using a leapfrog-type Verlet algorithm and the integration time step was set to 1 fs. The Berendsen thermostat[70] with a temperature relaxation time of 0.5 ps was also used to constrain the temperature during the simulations. The molecular geometry of the species was also constrained by using the SHAKE method.[71]

The selected potential models employed to simulate sc CO$_2$, CH$_3$OH, and H$_2$O were the EPM2,[72] OPLS-UA (J2),[73] and the SPC/E,[74] respectively. These models have been presented in our previously published works, and their selection has been justified therein.[61,62] The simulation of sc NH$_3$ was based on a 4-site potential model[75] consisting of Lennard−Jones (LJ) plus coulomb electrostatic terms. The model used is due to Kristof et al. (model 3 in ref 75), obtained by optimizing the previous Impey−Klein potential[76] in order to calculate the system properties along the vapor−liquid coexistence curve. Trial MD runs of this fluid with the optimized potential model provided accurate results for the pressure of the system for all the investigated densities along the simulated isotherm. The potential models employed to simulate sc CH$_4$ (OPLS-AA),[7] sc N$_2$,[78] and sc Xe[69] have been found to be very accurate in predicting certain properties of these fluids[65,69] in a wide range of the sc P,V,T phase space. In each simulation, a cutoff radius of 1.2 nm has been applied for all the LJ interactions, and long-range corrections have been also taken into account. For the cross potential interaction terms, the Lorentz−Berthelot combining rules were used. Moreover, to account for the long-range electrostatic interactions the Ewald summation technique was used, based on the Newton−Gregory forward difference interpolation scheme.

III. Results and Discussion

A. Local Intermolecular Structure. *Static LDIs.* The local intermolecular structure of all the investigated scfs has been studied in detail by analyzing the molecular trajectories obtained and then calculating the appropriate pair radial distribution functions (prdfs) $g(r)$. The center of mass (com) prdfs for some representative state points from state A to I (see Table 1) of sc H$_2$O, MeOH, and CO$_2$ may be found in our previous studies,[61,62] whereas those for sc NH$_3$ and N$_2$ are presented in the Supporting Information.

To obtain information about the LDIs and the average local densities around the species in the fluids, we have calculated the effective local densities, $\rho_{eff,l}$,[61,62] and from them the LDA, $\Delta\rho_{eff,l} = \rho_{eff,l} - \rho$, as well as the enhancement factors, $\rho_{eff,l}/\rho$ (ρ is the bulk density). The calculation of these properties is based upon the coordination numbers, $N_{co} = f(\rho)$, obtained each time from the corresponding com prdfs. An analytic description and justification of the use of this specific methodology applied to investigate LDI effects in scfs may be found in our published

Physicochemical Properties of Supercritical Fluids

J. Phys. Chem. B, Vol. 113, No. 9, 2009 **2785**

TABLE 3: Cutoff Distances for the First and Second Shell of Each Investigated System at the Reference Density $\rho_{ref} = 2\rho_c$

system	first shell cutoff (nm)	second shell cutoff (nm)
Xe	0.636	1.046
CH_4	0.590	0.970
CO_2	0.600	0.950
N_2	0.578	0.963
NH_3	0.526	0.864
CH_3OH	0.630	1.010
H_2O	0.422	0.675

papers,[61,62] as well as in other previous studies.[46,57] The reference density, ρ_{ref}, employed for the calculation of the effective local densities and corresponding quantities (see eq 2 in ref 61) has been set equal to $2\rho_c$. Moreover, the cutoff distances used in all the simulated state points to calculate these quantities correspond to the position of the first and second minimum of each com prdf at the reference (liquid-like) density are presented in Table 3. Note that these distances correspond to the radii characterizing the first and second solvation shell of the molecules in each fluid at the PVT state points under investigation.

The average coordination numbers, $N_{co} = f(\rho)$, for the first and second shell (some of them are shown later in Figure 4) of a particle up to a distance R_c obtained for each investigated fluid at the same isotherm, $T/T_c = 1.03$, clearly show a nonlinear density dependence. By inspecting more precisely these numbers in the first shell, we may observe that the convexity in $N_{co}(\rho)$ is different from one fluid to another. It seems to be apparently
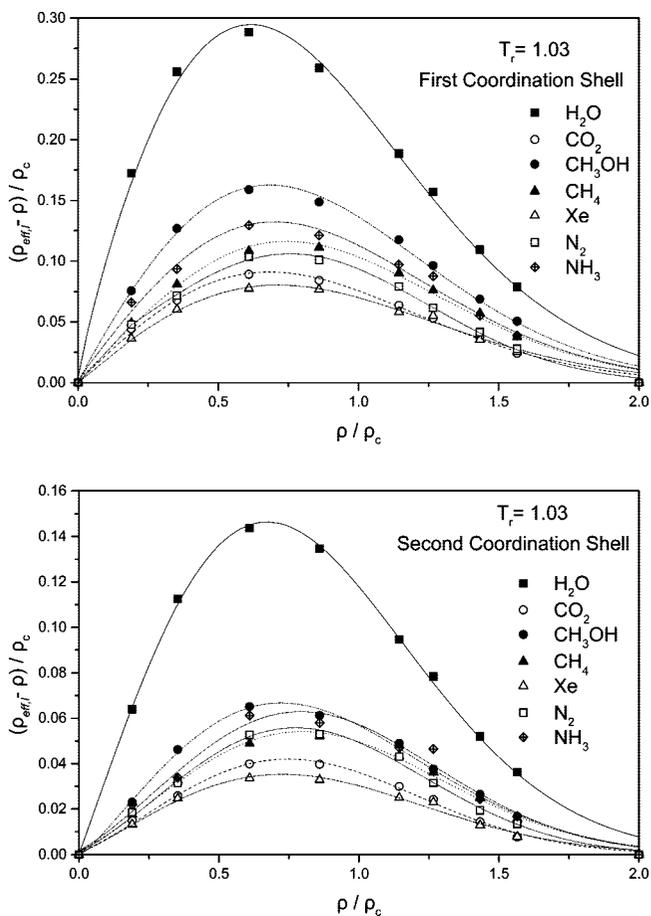
Figure 1. Local density augmentation (LDA) for the first and second coordination shell of the supercritical fluids under investigation against the density. The lines correspond to the fitted Weibull functions.
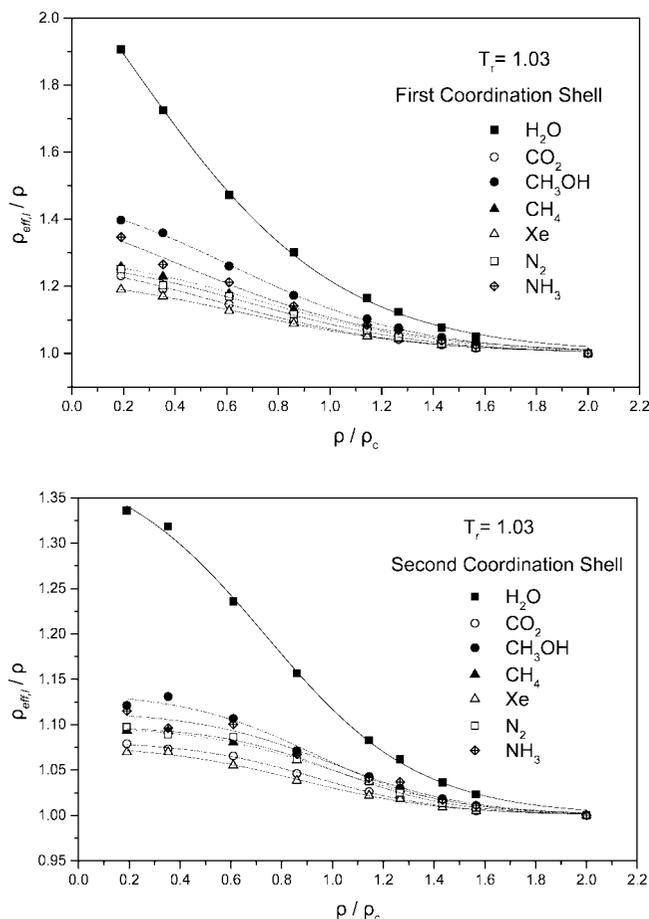
Figure 2. Local density enhancement factors for the first and second coordination shell of the supercritical fluids under investigation against the density.

greater in the case of the HB fluids H_2O, MeOH, and NH_3 compared to the nonassociated ones, namely, CO_2, N_2, CH_4, and Xe. Concretely speaking, in view of the above we clearly see that the slopes of the coordination numbers N_{co} at the low-density region are quite different from one fluid to another, increasing in the following order: sc Xe < sc CO_2, sc CH_4, sc N_2 < sc NH_3 < sc MeOH < sc H_2O. This result seems to be consistent with the well-known fact that N_{co} of the fluids at low densities is governed by the energy factor, as pointed out previously.[51b] In addition, as mentioned above this feature is directly related to the LDI effects and indicates the presence of a somewhat LDA or enhancement on average around a tagged molecule in each scf under study. Thus, in each case we have calculated the reduced LDA values, $\Delta\rho_{eff,l}/\rho_c$, for the first and second solvation shell of the investigated scfs and the results are shown in Figure 1, whereas the corresponding enhancement factors are shown in Figure 2. Note that the smooth curves in both figures represent the best fits of the simulated data to a four-parameter Weibull line shape function and sigmoidal Boltzmann one (see eq 6 and text in ref 62), respectively.

The parameter values obtained for these model functions for the first shell of each system are shown in Table 4. From Figures 1 and 2 and Table 4, we may easily draw some general remarks. First of all, it is clearly seen that the LDA and local density enhancement is more pronounced in dipolar and HB fluids in comparison with the other investigated quadrupolar and octupolar ones, signifying in this way the effect of the strong dipole−dipole interactions upon the formation of more cohesive local intermolecular structures with enhanced local densities.
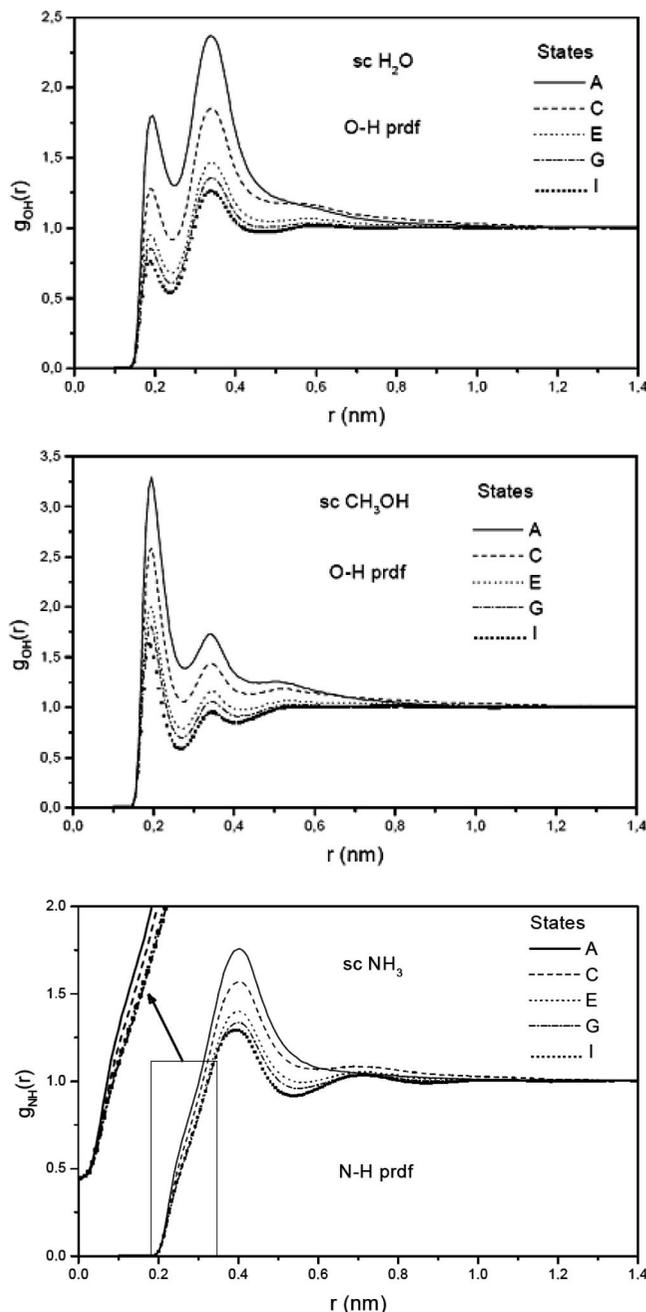
Figure 3. Site−site pair distribution functions of sc H_2O, sc MeOH, and sc NH_3 between atoms involved in hydrogen bonds (O···H for H_2O−H_2O and MeOH−MeOH, N···H for NH_3−NH_3).

Additionally, we do not find significant differences among the LDA magnitudes of the investigated quadrupolar (N_2, CO_2) and octupolar (CH_4) scfs. Concerning finally the inert monatomic sc Xe, we may observe even weaker LDI effects in comparison with all the other molecular fluids studied. All these observations signify the strong influence of the polarity of the molecules, when present, on the formation of LDIs in the sc state.

From an experimental point of view, the determination of local densities in molecular fluids is usually detected indirectly by spectroscopically measuring some molecule-centered observable quantity that is sensitive to the fluid's local density around it.[4,46] Up to now, several sets of such spectroscopic measurements have been reported in the literature devoted to the estimation of LDI effects for a limited number of pure scfs. Among these studies we mention those results reported for sc MeOH and sc CO_2. Note, finally, that any comparison and

TABLE 4: The Fitted Parameters of the Weibull and Sigmoidal Boltzmann Functions, Corresponding to Local Density Augmentation and Enhancement Factors for a Cutoff Distance Corresponding to the First Shell of Each Investigated System[a]

| system | Weibull parameters | | | |
	a	b/ρ_c	c	ρ_0/ρ_c
Xe	0.080	1.023	1.976	0.713
CH_4	0.116	1.038	2.082	0.744
CO_2	0.091	0.974	1.989	0.683
N_2	0.106	1.213	2.661	0.756
NH_3	0.132	1.004	2.003	0.701
CH_3OH	0.163	0.986	1.957	0.683
H_2O	0.295	0.941	1.849	0.615

| system | sigmoidal Boltzmann parameters | | |
	a'	b'/ρ_c	ρ_0'/ρ_c
Xe	1.242	0.362	0.661
CH_4	1.313	0.363	0.725
CO_2	1.309	0.368	0.566
N_2	1.297	0.346	0.698
NH_3	1.532	0.422	0.416
CH_3OH	1.517	0.354	0.626
H_2O	2.721	0.399	0.230

[a] See Table 3.

discussion of the MD predictions for LDA of pure sc H_2O, sc NH_3, and the rest of the fluids studied in the present work with corresponding results from suitable experiments is impossible due to the lack of such experimental information up to now.

In the case of neat sc MeOH, Saitow et al.[19] reported spectroscopic measurements focused on the estimation of LDA as a function of the density. According to their results, the LDA of this fluid is more pronounced than those observed for simple non-HB fluids. Note that the aforementioned results in comparison with our predictions were thoroughly discussed in a previous MD study of this fluid.[62] The main issue coming out from that study is that at a particular density of the fluid, the LDA estimated from the band center measurements is sensitive upon the selection of the vibrational mode used to characterize it. Furthermore, the expected nonlinear dependence of the spectral shifts and widths from the density should be taken into account in the methodology used.

More recently, Cabaco et al.[39] employed Raman spectroscopy to study the line shifts and widths of the Fermi dyad (1285 and 1388 cm⁻¹) in sc CO_2. The authors estimated the LDA of the fluid along the isotherm 307 K, which is quite close to 313 K employed by us in the MD study of this fluid. As pointed out in that study, the LDA obtained are sensitive on the investigated vibrational mode, as well as the methodology used to analyze the spectra recorded. More specifically, in their treatment the authors fitted each component of the dyad band shapes using single- and double-Lorentzian profiles, with the latter representing better the experimental band shapes at densities lower than $1.7\rho_c$. Further to this, their results for LDA were directly compared with our MD predictions[62] (see Figure 8d in ref 39), and it is noticeable to note that they are found to be in good agreement with each other.

Static LDIs and Hydrogen Bonding. In what follows, we will discuss the LDA effects observed in the case of sc H_2O, MeOH, and NH_3 together with the corresponding $N_{co}(\rho)$ and the H-bonding network in the fluids throughout the entire density range. As a first step toward exploring a possible interrelation between the HB nature of these fluids and the formation of LDIs, from Figures 1 and 2 we may observe that the magnitude of

Physicochemical Properties of Supercritical Fluids

J. Phys. Chem. B, Vol. 113, No. 9, 2009 **2787**
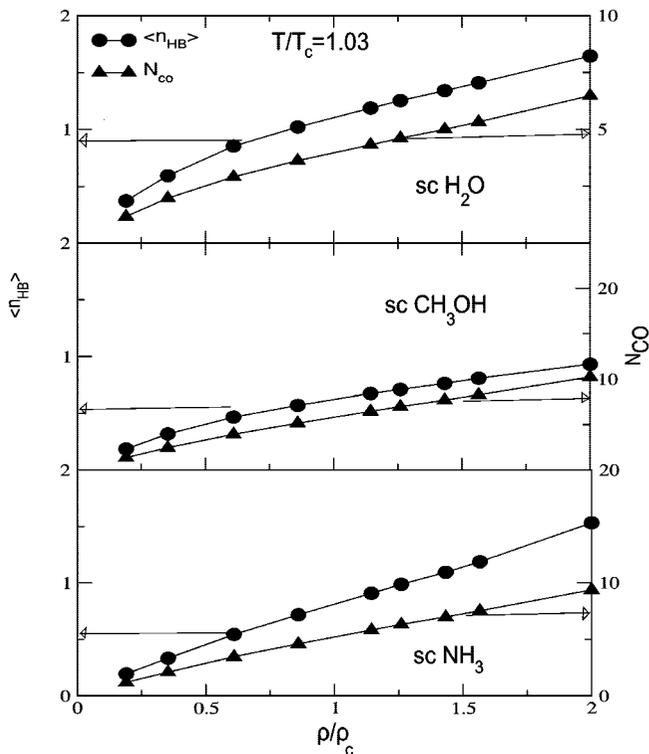
Figure 4. The density dependence of the calculated coordination numbers $N_{co}(\rho)$ corresponding to the first shell cutoff and mean number of H-bonds per molecule $\langle n_{HB} \rangle$ for sc H_2O, sc MeOH, and sc NH_3 from this MD study.

LDA and local density enhancement in sc H_2O, a strong HB molecular system even at sc conditions, is significantly pronounced compared with sc MeOH and NH_3, which are significantly weaker HB fluids than sc H_2O. The HB nature of these compounds at sc conditions has been systematically reported in a number of previous experimental[79−81] and simulation[67a,82] studies. Note furthermore that these features might also be qualitatively observed by the shape (at very short correlation distances) of the appropriate site−site O⋯H and N⋯H prdfs of these fluids shown in Figure 3. Concretely, the O⋯H prdfs for sc H_2O and CH_3OH exhibit a common feature at very short distances around 0.2 nm, namely the existence of a sharp-peaked first maximum followed by a deep minimum at an almost unchanged distance going from very low (state A) to liquid-like densities (state I). This characteristic behavior may be generally regarded as an indication of hydrogen bonding, as also pointed out in previous studies of both fluids at other sc conditions. This is also confirmed by the hydrogen-bonding analysis presented below.

From the same figure, the N⋯H prdf shows the presence of both H-bonded and non-H-bonded H atoms in the first solvation shell of NH_3. The shoulder up to about 2.7 Å can be attributed to hydrogen-bonded H atoms, whereas the more pronounced peak at a larger distance around 4.0 Å corresponds to the hydrogen atoms in the solvation shell that are not hydrogen bonded. We mention here that such a characteristic HB local structure has been also found first for liquid NH_3 both experimentally as well as theoretically.[84] A more detailed analysis of HBs in sc NH_3 at the aforementioned conditions is given below.

With the aim to obtain a more detailed picture of the HB network in these fluids at sc conditions of interest, we performed an analysis based upon well-known criteria. In the case of sc H_2O, we have applied a commonly used criterion, according to

which[83] a hydrogen bond between two water molecules exists if the interatomic distances are $R_{O\cdots O} \leq 0.36$ nm, $R_{H\cdots O} \leq 0.24$ nm, and the angle $H-O\cdots O \leq 30°$. For sc MeOH, we applied the criterion used in our previous studies,[67a] according to which a hydrogen bond between two methanol molecules exists if the interatomic distances are such that $R_{O\cdots O} \leq 0.35$ nm, $R_{H\cdots O} \leq 0.26$ nm, and the angle $H-O\cdots O \leq 30°$. Note that the estimated average number of hydrogen bonds per methanol molecule $\langle n_{HB} \rangle$ was found in good agreement with experiment in a wide range of sc conditions. Finally, in the case of sc NH_3 we used the criterion suggested by Boese et al.,[84] according to which two molecules are hydrogen bonded if $R_{N\cdots H} \leq 0.27$ nm and $R_{N\cdots N} \leq 0.525$ nm. In view of the above, the calculated $\langle n_{HB} \rangle$ for sc H_2O, MeOH, and NH_3 are presented in Figure 4. Note that in each case $\langle n_{HB} \rangle$ has been estimated independently on whether the molecule participates in a bond as a donor or acceptor. Moreover, this figure shows the density dependence of the coordination numbers $N_{co} = f(\rho)$ for the first shell of the particles in the HB fluids studied. Note also that our calculations have been extended to incorporate hydrogen-bond statistics, by estimating the percentage distribution f_i of molecules with i ($i = 0, 1, 2, 3...$) bonds per molecule, where f_0 denotes the percentage of no bonded molecules or monomer, f_1 the percentage of the molecules with one H-bond, etc. These distributions are presented in Figure 5.

Let us now reconsider the estimated reduced LDA and enhancement factor values of the three associated scfs. As shown in Figures 1 and 2, the results for sc H_2O are almost twice greater compared to those for sc MeOH, whereas those for sc NH_3 remain somewhat lower than the previous ones. We recall here that the estimated excess local density, $\Delta\rho_{eff,l}$, of these fluids as a function of density is augmented above ρ generally for densities smaller than $1.6\rho_c$. Moreover, one should also keep in mind that the predicted maximum LDA values of these scfs for the first shell, summarized in Table 4, are observed in the range from 0.61 to $0.75\rho_c$. Specifically, for sc H_2O the maximum LDA value for the first shell is observed at $0.615\rho_c$, whereas for sc MeOH and sc NH_3 at $\rho = 0.683\rho_c$ and $0.701\rho_c$, respectively.

Of course, this difference among the LDA values of these fluids becomes most significant at the density range of the fluids where their LDA effects are attained to be the greatest ones. It becomes clear from the observations above that there is need of a comprehensive understanding of these LDA results. For example, an open question here is whether the observed quite different LDA effects among these associated scfs is a consequence of the relative different strength of interactions, especially the attractive ones, between the species in the first coordination shell or/and the induced molecular ordering (or molecular packing) due to different HB network of these scfs.

To this point and according to the results obtained, one easily sees that despite the fact that the magnitudes of the dipole moments corresponding to the SPC/E model for H_2O and OPLS-UA (J2) for MeOH used in this study are quite close to each other (2.35 and 2.22 D, respectively), the LDA magnitudes of these scfs are found to be fairly different to each other. This consideration signifies the fact that, except for the polarity of the species in a scf, its characteristic HB network, when present, seems to also be a crucial factor in the formation of LDIs. A similar conclusion can also be indirectly drawn from a careful contrast between the coordination numbers $N_{co} = f(\rho)$ and the average number $\langle n_{HB} \rangle$ of these scfs shown in Figure 4. As mentioned already above, the deviation of $N_{co} = f(\rho)$ from a

2788 *J. Phys. Chem. B, Vol. 113, No. 9, 2009*

Skarmoutsos et al.
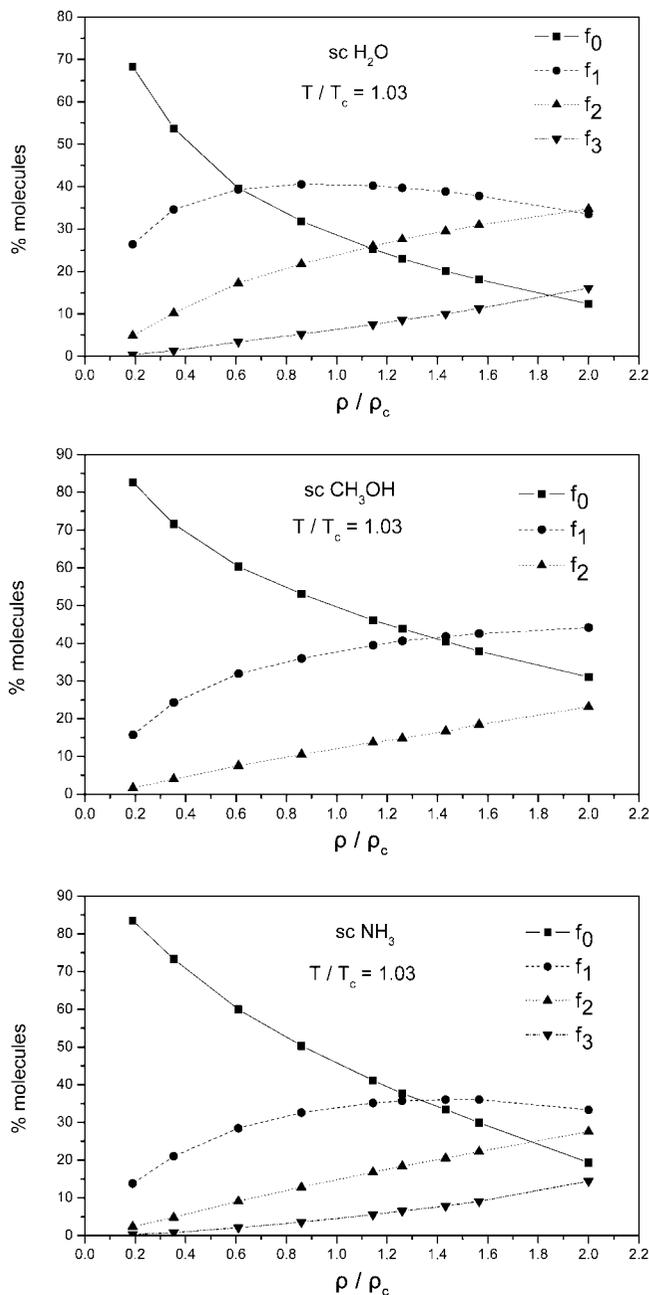
Figure 5. The density dependence of the calculated percentage distribution f_i of molecules with ($i = 0, 1, 2, 3$) H-bonds per molecule, for sc H_2O, sc MeOH, and sc NH_3 from this MD study.

linear density dependence is different from one fluid to another and appears to be particularly greater in the case of sc H_2O compared to sc MeOH, sc NH_3 and of course to the nonassociated scfs studied here. From the same figure, by carefully inspecting the density dependence of the HB numbers $\langle n_{HB} \rangle$ of the three fluids we may observe that in each case their behavior with density provides some similitude with that obtained for the corresponding coordination numbers $N_{co} = f(\rho)$. In fact, we may also observe a nonlinear behavior of the HB numbers $\langle n_{HB} \rangle$ at low and intermediate densities, which in the case of sc H_2O is much more pronounced in comparison with sc MeOH and NH_3. To analyze these results in detail, it is of particular interest to examine the percentage distribution f_i of molecules with i ($i = 0, 1, 2, 3...$) bonds per molecule obtained for these fluids, presented in Figure 5. In this figure, the values obtained for the percentage distribution f_i are plotted against the entire densities of the fluids studied. By precisely inspecting these results, we

easily see that the corresponding percentage distribution f_i of each HB fluid fall on different curves with increasing ρ/ρ_c. Concretely, from the results obtained for f_o (percentage of monomer) of scfs H_2O, MeOH, and NH_3, we may observe in general that they decrease with increasing density ρ/ρ_c. We note, however, that the percentage of the free or monomer molecules in sc MeOH, and to an almost similar extent in sc NH_3, are significantly higher compared to those in sc H_2O for densities in the range $0.2-2.0\rho_c$. This outcome is qualitatively in agreement with the aforementioned result concerning the density dependence of the mean number of H-bonds per molecule $\langle n_{HB} \rangle$ found for the three associated scfs.

Further to this, as noted in previous studies devoted in the field of H-bonding network forming in associated fluids, the degree of H-bonding aggregation is different for each system. It strongly depends upon the ability of neighboring molecules to form cooperative network rearrangement of multiple lengths with different number of molecules, due to the strong, local anisotropic interactions. As for the case of liquid water, for instance, it is well-known from previous studies that each tagged molecule can form at most four H-bonds. This results not only in a three-dimensional but also in an open locally tetrahedral network intermolecular structure. On the other hand, in the case of liquid CH_3OH, each molecule can form at most three H-bonds, and only one can be characterized as the proton donor. Generally, previous experimental studies have shown that the mean number of H-bonds per CH_3OH molecule in the liquid state is two. In other words, on the basis of the above considerations one may conclude that liquid CH_3OH molecules form more linear chains, rather than a three-dimensional network such as liquid H_2O. At this point, it is also interesting to mention that, as evidenced by a number of experimental and simulation studies, the mean number of H-bonds per molecule $\langle n_{HB} \rangle$ in H_2O and CH_3OH decreases with increasing temperature and decreasing density.[67a,85,86,89] On the other hand, high temperature spectroscopy experiments have shown that the H-bonding persists above the critical temperature of H_2O and CH_3OH.[85,87,88] Also, the H-bonded network in sc H_2O is formed by finite molecular aggregates. To this particular problem, the size of H-bond clusters in H_2O and CH_3OH has been investigated for a number of thermodynamic states, including sc conditions by computer simulation.[67a,82,88] The main outcome from all the above previous studies might be summarized in the fact that both fluids at sc conditions remain highly structured due to the existence of the H-bonds network among the molecules in this state. However, the strong local coupling of the individual sites, especially among the H_2O molecules, lead to the existence of a more compact H-bond network at sc conditions compared to the sc MeOH and NH_3. This interesting result may be easily drawn from our calculations concerning the percentage of molecules in sc H_2O, MeOH, and NH_3 participating in one (f_1), two (f_2), three (f_3), etc., H-bonds, shown in Figure 5 as a function of the system density. Concretely speaking, by inspecting the behavior of the percentage f_1 for the three fluids we may observe that the results for sc H_2O are significantly higher than those for MeOH and NH_3. Also, another interesting result is the behavior of the percentage f_2, which in the case of sc H_2O is much higher than those of MeOH and NH_3. Finally, the present analysis based on the H-bond statistics reveals the main reason why in the range of $0.6-0.85\rho_c$ the mean number of HBs for scH_2O is higher than that of scMeOH and scNH_3. This fact results in a more compact H-bond network close to a tagged molecule in water compared to MeOH and NH_3. This outcome

Physicochemical Properties of Supercritical Fluids

J. Phys. Chem. B, Vol. 113, No. 9, 2009 **2789**
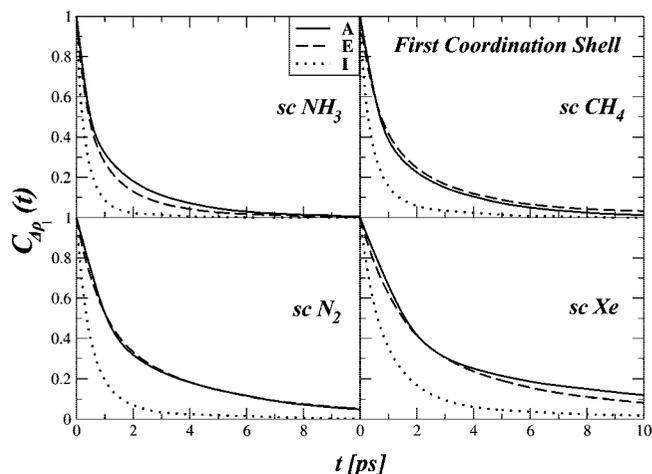
Figure 6. The calculated local density tcfs $C_{\Delta\rho_l}(t)$ for the first coordination shell of molecules in scfs Xe, N_2, CH_4, and NH_3 at state points A, E, and I.
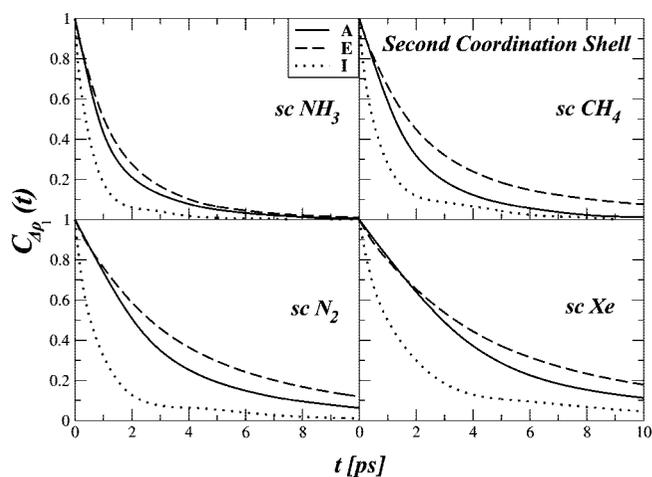
Figure 7. The calculated local density tcfs $C_{\Delta\rho_l}(t)$ for the second coordination shell of molecules in scfs Xe, N_2, CH_4, and NH_3 at state points A, E, and I.

might be characterized as the main origin of an increased LDA effect in the case of sc H_2O.

B. Local Density Reorganization Dynamics. The local density dynamics in all the scfs studied here were investigated on the basis of the appropriate time correlation functions (tcfs), $C_{\Delta\rho_l}(t)$.[40,61,62] By analyzing this correlation it is possible to determine the local density reorganization times $\tau_{\Delta\rho_l}$ around the molecules in a fluid at each thermodynamic state point. The tcfs for sc H_2O, MeOH, and CO_2 may be found in our previous papers,[61,62] whereas some representative plots of these functions for the first and second coordination shell of sc NH_3, N_2, CH_4, and Xe are presented in Figures 6 and 7, respectively. By carefully inspecting the time decay of these tcfs, we may draw some general conclusions. First of all, the time required for $C_{\Delta\rho_l}(t)$ approaching zero decreases with increasing density, and this time also is larger in the case of the second coordination shell in comparison with the first one. In general, the shape of these functions changes significantly from low to high densities for both coordination shells, signifying in this way the density effect upon the dynamics of the local environment around each molecule.

We recently proposed[62] that the time-decay of $C_{\Delta\rho_l}(t)$ for the first shell could be very well represented by a model function consisting of two separate components of the form:

$$C_{\Delta\rho_l}(t) = C_1(t) + C_2(t) = c\mathrm{e}^{-t/t_1} + (1-c)\mathrm{e}^{-t/t_2} \quad (1)$$

More specifically, we found that the local density reorganization for the first shell of the molecules in sc CO_2 and MeOH involves two relaxation processes, namely one responsible for the short-time dynamics and the other describing the long-time behavior. The results obtained in the present study have also been found to be in agreement with our previous findings, confirming our previous statement that the local density reorganization process at very short length scales (first shell) in pure molecular scfs could be described through two different reorganization "modes", a slow mode and a fast one.

The analysis of $C_{\Delta\rho_l}(t)$ in two component functions as some representative plot is shown for state point A of sc NH_3 in Figure 8. From the log scale plotting of $C_{\Delta\rho_l}(t)$ in this figure its biexponential behavior is clearly seen. In addition, as pointed out quite recently for sc CH_3OH and CO_2, similarly here the acf $C_1(t)$ contributes mainly to the shape of $C_{\Delta\rho_l}(t)$ at relatively small time scales and decays to zero quite fast, whereas $C_2(t)$ contributes mainly at larger time scales and decays to zero quite slower than $C_1(t)$. In the whole density range (not shown here), the values of $C_1(0)$ are significantly larger than the corresponding $C_2(0)$ ones. At the high-density region the values of $C_1(0)$ increase with increasing density, whereas the values of $C_2(0)$ exhibit the opposite behavior and decrease more rapidly than even in the case of sc CO_2. This finding indicates that the contribution of the slow relaxation processes in the local environment reorganization mechanism becomes very weak at the high bulk density region. Note finally that a similar behavior has been found for the local density reorganization process that has taken place in the rest of the scfs under investigation.

The local density reorganization time $\tau_{\Delta\rho_l}$ can also be expressed by the sum of two different relaxation times, τ_1 and τ_2:

$$\tau_{\Delta\rho_l} = ct_1 + (1-c)t_2 = \tau_1 + \tau_2 \quad (2)$$

A complete listing of the calculated values of c, t_1, and t_2 for sc H_2O, NH_3, N_2, CH_4, and Xe is provided for all the investigated state points in Tables S1–S5 of the Supporting Information. The bulk density dependence of τ_1, τ_2, and $\tau_{\Delta\rho_l}$ is presented in Figures 9 and 10. The corresponding values obtained for sc CO_2 and CH_3OH may also be found in our previous study (see ref 62).

By inspecting the bulk density dependence of all the aforementioned relaxation times, we may observe that the τ_1 values are significantly smaller than the τ_2 ones for the region of low densities and up to $1.2\rho_c$. In the high-density region the τ_2 values decrease monotonically with density, whereas the relaxation time τ_1 remains almost constant in the whole density range. The density dependence of the total local density reorganization time $\tau_{\Delta\rho_l}$ for the first shell shows a similar trend with the density dependence of the relaxation time τ_2.

Note furthermore a constant monotonic decrease of $\tau_{\Delta\rho_l}$ with density that is much more pronounced in the case of sc H_2O and MeOH, as well as to a somewhat lower degree for sc NH_3, than in the investigated non-dipolar and non-HB fluids. This behavior might be interpreted in terms of the bulk density effect upon the HB structure and dynamics in the associated fluids. It is pointed out recently that as the bulk density increases along an isotherm the lifetime of the hydrogen bonds decreases.[82d] Such a behavior might be explained in terms of the increase of the collisional events among the HB molecules, leading to a
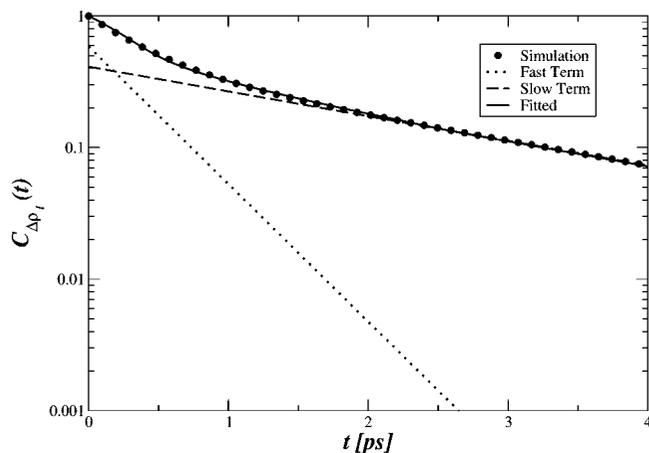
Figure 8. The analysis of the calculated total local density tcfs $C_{\Delta\rho_l}(t)$ for the first shell of molecules in sc NH_3 in two component functions $C_1(t)$ and $C_2(t)$ according to the well-fitted model function (see eq 1) for the representative state point A of the fluid.
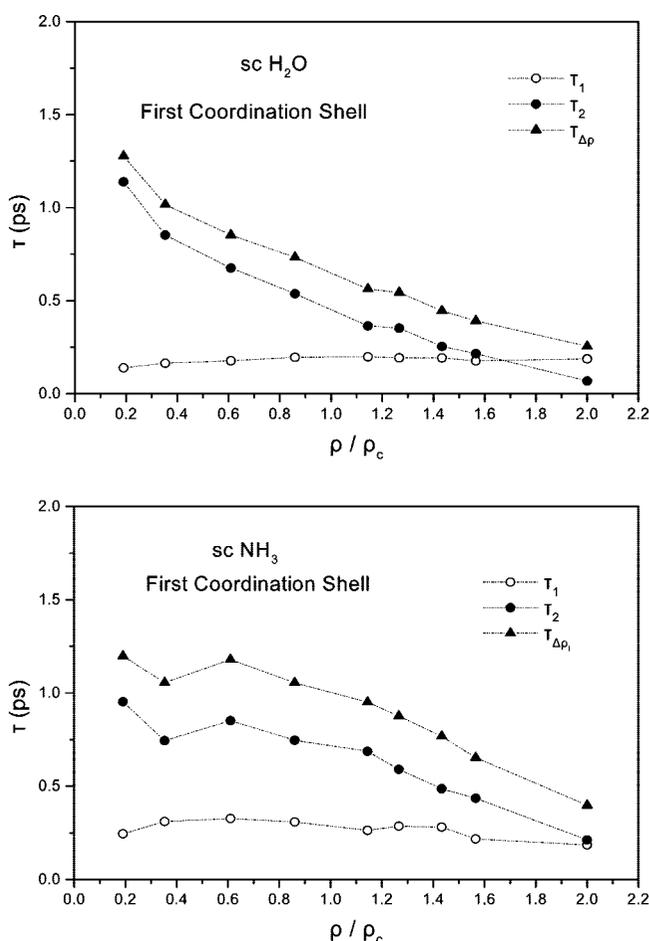
Figure 9. The density dependence of the calculated correlation times $\tau_{\Delta\rho_l}$, τ_1, and τ_2 corresponding to the tcfs $C_{\Delta\rho_l}(t)$, $C_1(t)$, and $C_2(t)$ for the first shell of sc H_2O and sc NH_3 from this MD study.

more frequent breaking of hydrogen bonds and, eventually, to a faster local density reorganization process at the high bulk density region. Previous MD simulations of sc H_2O by Guardia and Marti[90] also support this fact, where the residence times of the water molecules were calculated for a wide density range along several sc isotherms. According to the authors in that study, the residence time for a water molecule in the first coordination shell decreases when going from the low- to high-density region. Therefore, at higher densities the molecules
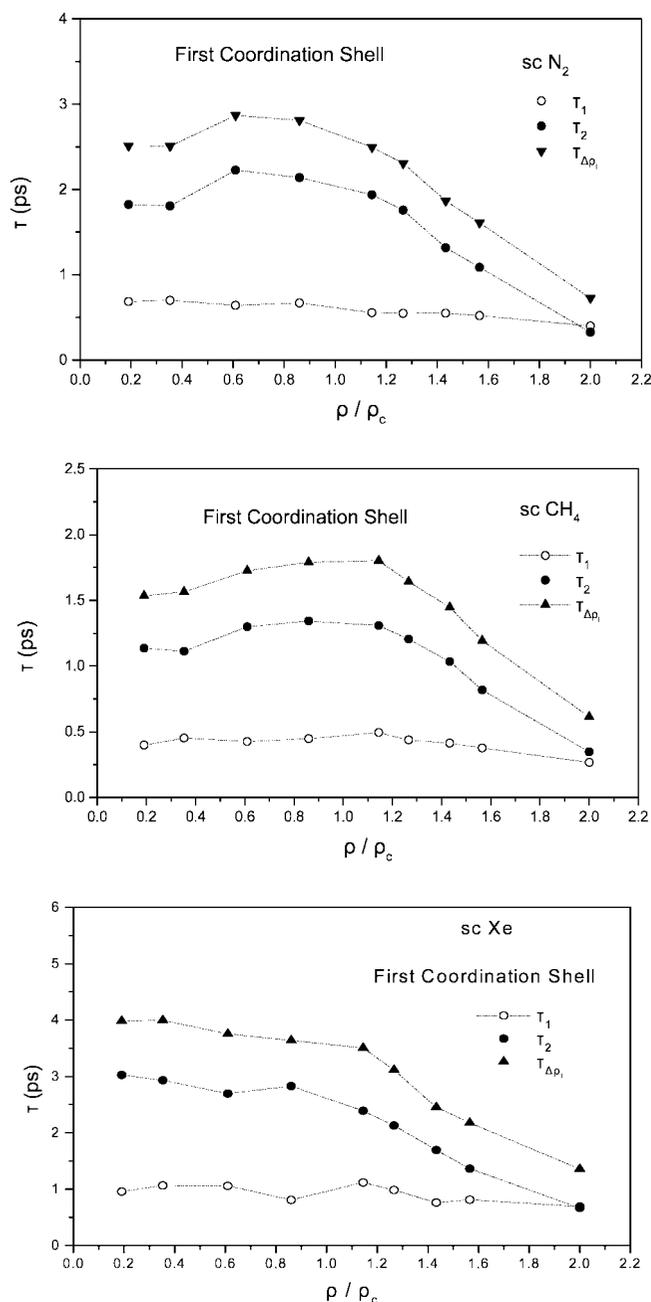
Figure 10. The density dependence of the calculated correlation times $\tau_{\Delta\rho_l}$, τ_1, and τ_2 corresponding to the tcfs $C_{\Delta\rho_l}(t)$, $C_1(t)$, and $C_2(t)$ for the first shell of sc N_2, sc CH_4, and sc Xe from this MD study.

migrate faster from the first to the second coordination shell, and subsequently, the whole local environment reorganization processes becomes faster. On the other hand, according to that study, the local intermolecular structure of water at low densities is that of a clustered fluid that has a diluted second coordination shell, therefore producing greater residence time values for the water molecules in the first shell. The formation of small metastable clusters[45] at the low-density region is, in general, a possible reason for this significant retardation in the local density redistribution.

It is very interesting to notice that in the present MD treatment when investigating the local density reorganization dynamics at larger distances around a tagged molecule, as in the case of the second coordination shell, the time decay of the tcfs $C_{\Delta\rho_l}(t)$, as well as their bulk density dependence, starts exhibiting a somewhat different behavior. The tcfs corresponding to the

Physicochemical Properties of Supercritical Fluids

J. Phys. Chem. B, Vol. 113, No. 9, 2009 **2791**
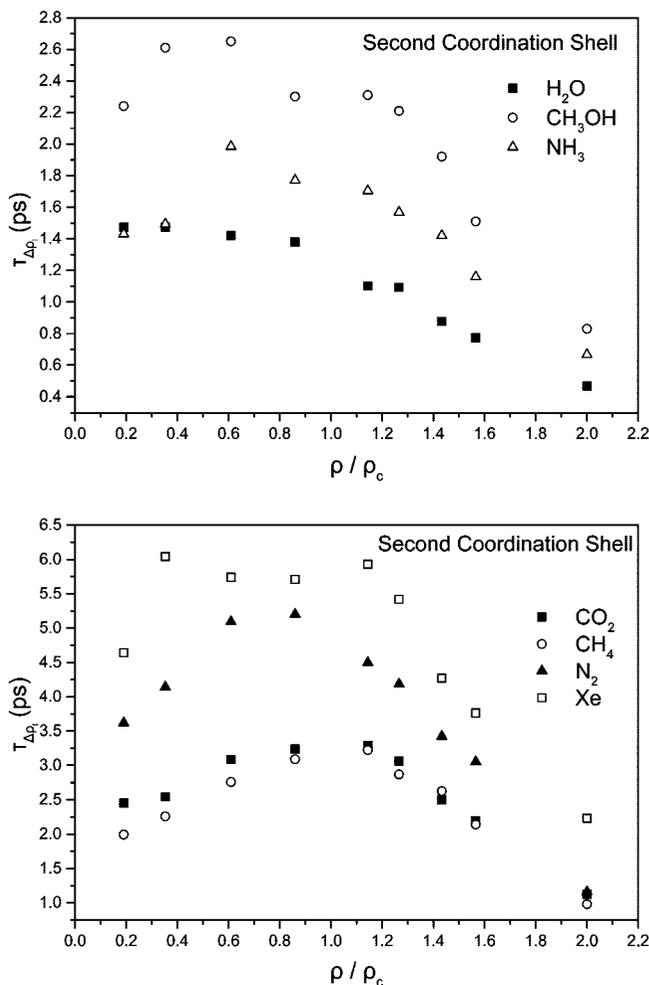
Figure 11. The density dependence of the calculated correlation times $\tau_{\Delta\rho_l}$ corresponding to the tcfs $C_{\Delta\rho_l}(t)$ for the second shell of all the scfs studied in this MD study.

second shell could not be well-fitted by the double exponential decay function (eq 1) proposed for the dynamics of the first one, especially at higher densities. This different behavior is much more clearly reflected on the density dependence of the calculated local density reorganization times $\tau_{\Delta\rho_l}$, especially in the case of nonpolar and non-HB scfs, depicted in Figure 11.

We may observe from the results shown in Figure 11 that, for the nonpolar and non-HB scfs, $\tau_{\Delta\rho_l}$ exhibits an increasing behavior that is maximized in the density region close to ρ_c. At higher densities, $\tau_{\Delta\rho_l}$ decreases significantly with density as in the case of the first shell dynamics. This trend is not observed only for the strong HB fluid water, indicating that the strong intermolecular interactions between the water molecules significantly affect not only the dynamics of the reorganization of the first solvation shell but also those corresponding to the second one. These strong intermolecular interactions may also be reflected on the positions of the first and second minimum of the com prdfs of water, which are located in shorter distances in comparison with the other not so strongly associated fluids (see Table 3).

A similar behavior has been observed in the two-dimensional study of Maddox et al.[45] by extending the length scale of the region around a central tagged particle. According to the authors in that study, this behavior might be explained by the fact that in the density region close to the critical one the critical fluctuations are maximized, causing by this way the increase of $\tau_{\Delta\rho_l}$, thus signifying the effect of the long-range "critical slowing down"[91] on local density dynamics.

The fact that for the larger solvation shell the values of $\tau_{\Delta\rho_l}$ tend to reach their maximum close to the critical density supports the previous mentioned findings, that at larger length scales the long-range fluctuations affect the local density dynamics. Of course, at even more extended length scales this phenomenon would be even clearer and would be more strongly related with long-range critical phenomena. However, even in the case of the second shell local density dynamics (which are local, short-range phenomena), we observe that this coupling between local end extended length scale collective phenomena arises and is more clearly seen for fluids with weaker intermolecular interactions. Therefore, it seems that the length scale where this coupling starts to affect the local density dynamics depends on the strength of the intermolecular interactions and presumably decreases with decreasing strength of the intermolecular forces. For polar strongly associated fluids, at these short-range length scales the dynamics of the reorganization of the first and second coordination shell are mainly controlled by the direct,[43] strong intermolecular interactions, and the indirect collective effects[43] presumably contribute more significantly at more extended length scales in comparison with nonpolar and non-HB scfs.

IV. Conclusions

The molecular dynamics simulation technique was used to investigate the features concerning the LDIs and their dynamics in various pure scfs, giving emphasis to the effect of the strength and special characteristics of the intermolecular interactions in these fluids upon these properties. The scfs under investigation have been chosen on the basis of the difference of the electrostatic character appearing in their intermolecular interactions, resulting from their different multipole expansion. More specifically, we have chosen to investigate some molecular systems representative for the following classes of scfs: monatomic, dipolar and hydrogen bonding (HB), quadrupolar, and octupolar. The selected investigation pure scfs are sc Xe, sc H_2O, sc NH_3, sc MeOH, sc CO_2, sc N_2, and sc CH_4. In the case of the dipolar scfs water, ammonia, and methanol, their HB nature was systematically explored and related to the behavior of the created local density inhomogeneities at all densities. The simulations were carried out along near-critical isotherms and for densities below and above the critical one.

The results obtained reveal strong influence of the dipolar and HB interactions of the investigated systems upon the local density augmentation (LDA). Concretely, the LDA and local density enhancement is more pronounced in dipolar and HB fluids in comparison with the other investigated quadrupolar and octupolar ones, whereas we do not find significant differences among the LDA magnitudes of the investigated quadrupolar (N_2, CO_2) and octupolar (CH_4) scfs. Finally, for the inert monatomic sc Xe, we may observe even weaker LDI effects in comparison with all the other molecular fluids studied.

Especially in sc H_2O, we found that the local density augmentation is sufficiently greater in comparison with all the other fluids, including also the HB ones NH_3 and MeOH, which might be attributed to the more compact H-bonding associative character of water. To investigate the effect of the HB network on the LDA, we performed a HB analysis in water, ammonia, and methanol. The results obtained reveal a nonlinear density dependence of the calculated average number of hydrogen bonds $\langle n_{HB} \rangle$, similar to that of the calculated coordination numbers N_{co}. In fact, this nonlinear behavior is much more pronounced in sc H_2O in comparison with sc MeOH and ammonia. In addition, taking into account that these molecules exhibit similar dipole moments, especially water and methanol, we may see

that the HB interactions in these fluids have a very strong effect on the formation of LDI, even stronger than the effect of the dipole−dipole interactions on these properties.

Concerning the dynamics of the local density reorganization in the investigated fluids, we have investigated the behavior of local density tcfs, $C_{\Delta\rho_l}(t)$, and the corresponding correlation times, $\tau_{\Delta\rho_l}$, as a function of the density and the radius of the shell around the molecules in each fluid. In general, the shape and time decay to zero as $C_{\Delta\rho_l}(t)$ changes significantly from low to high densities for the first and second shell of each fluid, signifying in this way the density effect upon the dynamics of the local density redistribution.

We have found that for each fluid under study our previously proposed[62] sum of two exponential decay functions might be considered as the most suitable one for the description of the characteristic features of the first shell redistribution dynamics. Thus, the correlation time $\tau_{\Delta\rho_l}$ could be expressed as the sum of two different correlation times. This behavior is more pronounced in the low-density region up to $1.2\rho_c$. This finding indicates for the first time that the description of the dynamical behavior of the local density redistribution around each molecule at short length scales (first shell) involves two relaxation processes, namely, one responsible for the short-time dynamics and the other one describing the long-time behavior. Furthermore, we have revealed that the contribution of the slow relaxation processes in the local environment reorganization mechanism becomes very weak at high bulk density. Note also that the observed constant monotonic decrease of $\tau_{\Delta\rho_l}$ with density is much more pronounced in the case of sc H_2O and MeOH, as well as to a somewhat lower degree for sc NH_3, than in the investigated non-dipolar and non-HB fluids.

Concerning the local density reorganization dynamics at larger length scales (second shell), we have revealed that, especially for the nonpolar and non-HB scfs, $\tau_{\Delta\rho_l}$ initially exhibits an increasing behavior with density maximized in the density region close to ρ_c. At higher densities, $\tau_{\Delta\rho_l}$ decreases significantly with density, as in the case of the first shell dynamics. It should be mentioned here that this trend is not observed in the case of the strong HB sc water, indicating also that the strong intermolecular interactions between the water molecules significantly affect not only the dynamics of the reorganization of the first solvation shell but also those corresponding to the second one. A possible reason for this is that, due to these interactions, the second shell of sc water is located at smaller distance in comparison with the other investigated fluids. In general, we may conclude that by increasing the length scale of the radius of a tagged molecule, the mechanism of the local density reorganization changes causing a maximization of $\tau_{\Delta\rho_l}$ close to the critical density and at short intermolecular distances this mechanism is much more apparent in fluids exhibiting weaker intermolecular interactions.

Supporting Information Available: A figure for the calculated com−com prdfs of sc NH_3 and N_2 at state points A-I is provided as Figure 1 of the Supporting Information. A complete listing of the calculated values of c, t_1 and t_2 appearing in eq 1 for scfs H_2O, NH_3, N_2, CH_4, and Xe is provided for all the investigated state points in Tables S1−S5 of the Supporting Information. This material is available free of charge via the Internet at http://pubs.acs.org.

References and Notes

(1) *Supercritical Fluids: Fundamentals and Applications*; Kiran, E.; Debenedetti, P. G.; Peters, C. J., Eds.; NATO ASI Science Series E, Applied Sciences; Kluwer Academic Publishers: Dordrecht, The Netherlands, 2000; Vol. 366.

(2) *Supercritical Fluid Science and Technology*; Johnston, K. P.; Kim, S.; Coumbes, J.; Penninger, J. M. L., Eds.; American Chemical Society: Washington DC, 1998; Ch. 5 and refs therein.

(3) Eckert, C. A.; Knutson, B. L.; Debenedetti, P. G. *Nature* **1996**, *383*, 313.

(4) Tucker, S. C. *Chem. Rev.* **1999**, *99*, 391.

(5) Besnard, M.; Tassaing, T.; Danten, Y.; Andanson, J. M.; Soetens, J. C.; Cansell, F.; Loppinet-Serani, A.; Reveron, H.; Aymonier, C. *J. Mol. Liq.* **2006**, *125*, 88.

(6) Kajimoto, O. *Chem. Rev.* **1999**, *99*, 355.

(7) (a) Lewis, J.; Biswas, R.; Robinson, A.; Maroncelli, M. *J. Phys. Chem. B* **2001**, *105*, 3306. (b) Sato, T.; Sugiyama, M.; Misawa, M.; Takata, S.; Otomo, T.; Itoh, K.; Mori, K.; Fukunaga, T. *J. Phys.: Condens. Matter* **2008**, *20*, 104203.

(8) Aizawa, T.; Kanakubo, M.; Ikushima, Y.; Smith Jr, R. L.; Saitoh, T.; Sugimoto, N. *Chem. Phys. Lett.* **2004**, *393*, 31.

(9) Okamoto, M.; Nagashima, H.; Tanaka, F. *Phys. Chem. Chem. Phys.* **2002**, *4*, 5627.

(10) Rice, J. K.; Niemeyer, E. D.; Dunbar, R. A.; Bright, F. V. *J. Am. Chem. Soc.* **1995**, *117*, 5832.

(11) Knutson, B. L.; Tomasko, D. L.; Eckert, C. A.; Debenedetti, P. G.; Chialvo, A. A. *Local Density Augmentation in Supercritical Solutions: A Comparison Between Fluorescence Spectroscopy and Molecular Dynamics Results. In Recent Advances in Supercritical Fluid Technology: Applications and Fundamental Studies*; Bright, F. V., McNally, M. E. P. Eds.; ACS Symposium Series; American Chemical Society: Washington, DC, 1992; Vol. 488, pp 60−72.

(12) Ben-Amotz, D.; LaPlant, F.; Shea, D.; Gardecki, J.; List, D. In *Recent Advances in Supercritical Fluid Technology: Applications and Fundamental Studies*; Bright, F. V., McNally, M. E. P. Eds.; ACS Symposium Series; American Chemical Society: Washington, DC, 1992; Vol. 488; pp 18−30.

(13) Nakayama, H.; Saitow, K.; Nakashita, M.; Ishii, K.; Nishikawa, K. *Chem. Phys. Lett.* **2000**, *320*, 323.

(14) Cabaco, M. I.; Besnard, M.; Tassaing, T.; Danten, Y. *Pure Appl. Chem.* **2004**, *76*, 141.

(15) Morita, T.; Kusano, K.; Ochiai, H.; Saitow, K.; Nishikawa, K. *J. Chem. Phys.* **2000**, *112*, 4203.

(16) Lalanne, P.; Tassaing, T.; Danten, Y.; Cansell, F.; Tucker, S. C.; Besnard, M. *J. Phys. Chem. A* **2004**, *108*, 2617.

(17) (a) Saitow, K.; Otake, K.; Nakayama, H.; Ishii, K.; Nishikawa, K. *Chem. Phys. Lett.* **2003**, *368*, 209. (b) Saitow, K.; Ohtake, H.; Sarukura, N.; Nishikawa, K. *Chem. Phys. Lett.* **2001**, *341*, 86.

(18) Saitow, K.; Nakayama, H.; Ishii, K.; Nishikawa, K. *J. Phys. Chem. A* **2004**, *108*, 5770.

(19) Saitow, K.; Sasaki, J. *J. Chem. Phys.* **2005**, *122*, 104502.

(20) Saitow, K.; Kajiya, D.; Nishikawa, K. *J. Phys. Chem. A* **2005**, *109*, 83.

(21) Saitow, K.; Kajiya, D.; Nishikawa, K. *J. Phys. Chem. A* **2005**, *109*, 7365.

(22) Saitow, K.; Kajiya, D.; Nishikawa, K. *J. Am. Chem. Soc.* **2004**, *126*, 422.

(23) Ruckenstein, E.; Shulgin, I. L. *Chem. Phys. Lett.* **2000**, *330*, 551.

(24) Betts, T. A.; Zagrobelny, J.; Bright, F. V. *J. Am. Chem. Soc.* **1992**, *114*, 8163. Heitz, M. P.; Maroncelli, M. *J. Phys. Chem. A* **1997**, *101*, 5852.

(25) Anderton, R. M.; Kauffman, J. F. *J. Phys. Chem.* **1995**, *99*, 13759.

(26) Heitz, M. P.; Bright, F. V. *J. Phys. Chem.* **1996**, *100*, 6889.

(27) deGrazia, J. L.; Randolph, T. W.; O'Brien, J. A. *J. Phys. Chem. A* **1998**, *102*, 1674.

(28) Bai, S.; Taylor, C. M. V.; Liu, F.; Mayne, C. L.; Pugmire, R. J.; Grant, D. M. *J. Phys. Chem. B* **1997**, *101*, 2923.

(29) Chen, S.; Miranda, D. T.; Evilia, R. F. *J. Supercrit. Fluids* **1995**, *8*, 255.

(30) Umecky, T.; Kanakubo, M.; Ikushima, Y. *J. Phys. Chem. B* **2003**, *107*, 12003.

(31) Cabaco, M. I.; Besnard, M.; Tassaing, T.; Danten, Y. *J. Mol. Liq.* **2006**, *125*, 100.

(32) Howdle, S. M.; Bagratashvili, V. N. *Chem. Phys. Lett.* **1993**, *214*, 215.

(33) Schwarzer, S.; Troe, J.; Zerezke, M. *J. Chem. Phys.* **1997**, *107*, 8380.

Physicochemical Properties of Supercritical Fluids

J. Phys. Chem. B, Vol. 113, No. 9, 2009 **2793**

(34) Schwarzer, S.; Troe, J.; Votsmeier, M.; Zerezke, M. *J. Chem. Phys.* **1996**, *105*, 3121.

(35) Benzler, J.; Linkersdörfer, S.; Luther, K. *J. Chem. Phys.* **1997**, *106*, 4992.

(36) Myers, D. J.; Urdahl, R. S.; Cherayil, B. J.; Fayer, M. D. *J. Chem. Phys.* **1997**, *107*, 9741.

(37) Urdahl, R. S.; Myers, D. J.; Rector, K. D.; Davis, P. H.; Cherayil, B. J.; Fayer, M. D. *J. Chem. Phys.* **1996**, *105*, 8973.

(38) Cherayil, B. J.; Fayer, M. D. *J. Chem. Phys.* **1997**, *107*, 7642.

(39) Cabaco, M. I; Longelin, S.; Danten, Y.; Besnard, M. *J. Phys. Chem. A* **2007**, *111*, 12966.

(40) Tucker, S. C.; Maddox, M. W. *; J. Phys. Chem. B* **1999**, *102*, 2437.

(41) Goodyear, G.; Maddox, M. W.; Tucker, S. C. *J. Chem. Phys.* **2000**, *112*, 10327.

(42) Goodyear, G.; Maddox, M. W.; Tucker, S. C. *J. Phys. Chem. B* **2000**, *104*, 6240.

(43) Maddox, M. W.; Goodyear, G.; Tucker, S. C. *J. Phys. Chem. B* **2000**, *104*, 6248.

(44) Goodyear, G.; Maddox, M. W.; Tucker, S. C. *J. Phys. Chem. B* **2000**, *104*, 6258.

(45) Maddox, M. W.; Goodyear, G.; Tucker, S. C. *J. Phys. Chem. B* **2000**, *104*, 6266.

(46) Song, W.; Biswas, R.; Maroncelli, M. *J. Phys. Chem. A* **2000**, *104*, 6924.

(47) Song, W.; Maroncelli, M. *Chem. Phys. Lett.* **2003**, *378*, 410.

(48) Husowitz, B.; Talanquer, V. *J. Chem. Phys.* **2007**, *112*, 054508.

(49) Perera, A. *J. Chem. Phys.* **2001**, *115*, 6115.

(50) Zhou, S. Q. *J. Phys. Chem. B* **2005**, *109*, 7522.

(51) (a) Egorov, S. A *J. Chem. Phys.* **2000**, *112*, 7138. (b) Egorov, S. A. *Chem. Phys. Lett.* **2002**, *354*, 140.

(52) Siavosh-Haghighi, A.; Adams, J. E. *J. Phys. Chem. A* **2001**, *105*, 2680.

(53) Egorov, S. A.; Yethiraj, A.; Skinner, J. L. *Chem. Phys. Lett.* **2000**, *317*, 558.

(54) Petsche, I. B.; Debenedetti, P. G. *J. Chem. Phys.* **1989**, *91*, 7075.

(55) Petsche, I. B.; Debenedetti, P. G. *J. Phys. Chem.* **1991**, *95*, 386.

(56) Petsche, I. B.; Debenedetti, P. G.; Mohamed, R. S. *Fluid Phase Equilib.* **1989**, *52*, 347.

(57) Nugent, S.; Ladanyi, B. M. *J. Chem. Phys.* **2004**, *120*, 874.

(58) Ruckenstein, E.; Shulgin, I. L. *J. Phys. Chem. B* **2000**, *104*, 2540.

(59) Debenedetti, P. G.; Chialvo, A. A. *J. Chem. Phys.* **1992**, *97*, 504.

(60) Egorov, S. A. *Chem. Phys. Lett.* **2002**, *354*, 140.

(61) Skarmoutsos, I.; Samios, J. *J. Phys. Chem. B* **2006**, *110*, 21931.

(62) Skarmoutsos, I.; Samios, J. *J. Chem. Phys.* **2007**, *126*, 044503.

(63) Skarmoutsos, I.; Dellis, D.; Samios, J. *J. Chem. Phys.* **2007**, *126*, 224503.

(64) Skarmoutsos, I.; Samios, J. *J. Mol. Liq.* **2006**, *125*, 181.

(65) Skarmoutsos, I.; Kampanakis, L. I.; Samios, J. *J. Mol. Liq.* **2005**, *117*, 33.

(66) Dellis, D.; Chalaris, M.; Samios, J. *J. Phys. Chem B* **2005**, *109*, 18575.

(67) (a) Chalaris, M.; Samios, J. *J. Phys. Chem. B* **1999**, *103*, 1161. (b) Chalaris, M.; Samios, J. *Pure Appl. Chem.* **2004**, *76*, 203.

(68) Chatzis, G.; Samios, J. *Chem. Phys. Lett.* **2003**, *374*, 187.

(69) Marinakis, S.; Samios, J. *J. Supercrit. Fluids* **2005**, *34*, 81.

(70) Berendsen, H. J. C.; Postma, J. P. M.; Van Gunsteren, W. F.; Di Nola, A.; Haak, J. R. *J. Chem. Phys.* **1984**, *81*, 3684.

(71) Ryckaert, J. P.; Ciccotti, G.; Berendsen, H. J. C. *J. Comp. Phys.* **1977**, *23*, 327.

(72) Harris, J. G.; Young, K. H. *J. Phys. Chem.* **1995**, *99*, 12021.

(73) Jorgensen, W. L. *J. Phys. Chem.* **1986**, *90*, 1276.

(74) Berendsen, H. J. C.; Grigera, J. R.; Straatsma, T. P. *J. Phys. Chem.* **1987**, *91*, 6269.

(75) Kristof, T.; Vorholz, J.; Liszi, J.; Rumpf, B.; Maurer, G. *Mol. Phys.* **1999**, *97*, 1129.

(76) Impey, R. W.; Klein, M. L. *Chem. Phys. Lett.* **1984**, *104*, 579.

(77) Jorgensen, W. L.; Maxwell, D. S.; Tirado-Rives, J. *J. Am. Chem. Soc.* **1996**, *118*, 11225.

(78) Cheung, P. S. Y.; Powles, J. G. *Mol. Phys.* **1975**, *30*, 921.

(79) (a) Postorino, P.; Tromp, R. H.; Ricci, M.-A.; Soper, A. K.; Nelson, G. W. *Nature (London)* **1993**, *366*, 668. (b) Soper, A. K. *Chem. Phys.* **2000**, *258*, 121. (c) Gorbaty, Y. E.; Kalinichev, A. G. *J. Phys. Chem.* **1995**, *99*, 5336.

(80) (a) Wernet, Ph.; Testernale, D.; Hazemann, J.-L.; Argoud, R.; Glatzel, P.; Pettersson, L. G. M.; Nilsson, A.; Bergmann, U. *J. Chem. Phys.* **2005**, *123*, 154503. (b) Bellissent-Funel, M.-C.; Tassaing, T.; Zhao, H.; Beysens, D.; Guillot, B.; Guissani, Y. *J. Chem. Phys.* **1997**, *107*, 2942. (c) Hoffmann, M. M.; Conradi, M. S. *J. Am. Chem. Soc.* **1997**, *119*, 3811.

(81) (a) Asahi, N.; Nakamura, Y. *Chem. Phys. Lett.* **1998**, *290*, 63. (b) Bai, S.; Yonker, C. R. *J. Phys. Chem. A* **1998**, *102*, 8641. (c) Yamaguchi, T.; Benmore, C. J.; Soper, A. K. *J. Chem. Phys.* **2000**, *112*, 8976.

(82) (a) Kalinichev, A. G.; Bass, J. D. *J. Phys. Chem.* **1997**, *101*, 9720. (b) Kalinichev, A. G.; Churakov, S. V. *Fluid Phase Equilib.* **2001**, *183*, 271. (c) Kalinichev, A. G.; Churakov, S. V. *Chem. Phys. Lett.* **1999**, *302*, 411. (d) Mizan, T. I.; Savage, P. E.; Ziff, R. M. *J. Phys. Chem.* **1996**, *100*, 403. (e) Asahi, N.; Nakamura, Y. *J. Chem. Phys.* **1998**, *109*, 9879. (f) Kiselev, M.; Kerdcharoen, T.; Hannongbua, S.; Heinzinger, K. *Chem. Phys. Lett.* **2000**, *327*, 425.

(83) (a) Nieto-Draghi, C.; Bonet Avalos, J.; Rousseau, B. *J. Chem. Phys.* **2003**, *118*, 7954. (b) Marti, J.; Padro, J.; Guardia, E. *J. Chem. Phys.* **1996**, *105*, 639.

(84) Boese, A. D.; Chandra, A.; Martin, J. M. L.; Marx, D. *J. Chem. Phys.* **2003**, *119*, 5965.

(85) Kalinichev, A. G.; Fugan, N. T.; Kubicki, J. D. *Reviews in Mineralogy and Geochemistry*; Mineralogical Society of America: Washington DC, 2001; Vol. 42, p 83.

(86) Hoffmann, M. M.; Conradi, M. S. *J. Phys. Chem. B* **1998**, *102*, 263.

(87) Bellissent-Funel, M. C. *J. Mol. Liq.* **2001**, *90*, 313.

(88) Mountain, R. D. *J. Chem. Phys.* **1999**, *110*, 2109.

(89) Kruse, A.; Dinjus, E. *J. Supercrit. Fluids* **2007**, *39*, 362.

(90) Guardia, E.; Marti, J. *Phys. Rev. E* **2004**, *69*, 011502.

(91) Binney, J. J.; Dowrick, N. J.; Fisher, A. J.; Newman, M. E. J. *The Theory of Critical Phenomena: An Introduction to the Renormalization Group*; Clarendon Press: Oxford, UK, 1993.